doi: 10.21860/medflum2022_284696

Hand model with dependency constrained joints for applications in rehabilitation robotics

Model šake s međuovisnim zglobovima za primjenu u rehabilitacijskoj robotici

Tomislav Bazina[1], Ervin Kamenar[1*], Saša Zelenika[1], Nelida Črnjarić-Žic[1], Tea Schnurrer-Luke-Vrbanić[2]

[1] University of Rijeka, Faculty of Engineering, Rijeka, Croatia

[2] University of Rijeka, Faculty of Medicine, Department for Physical and Rehabilitation Medicine, Rijeka, Croatia

Abstract. ***Aim:*** This work presents a method for developing a simplified but efficient model of the complex human hand kinematics with the aim of its implementation in rehabilitation robotics. ***Material and methods:*** The approach incorporates modularity by simplifying the available model comprising 24 degrees of freedom (DOFs) to 9 DOFs, with the introduction of additional joint coupling parameters specific to different grasp types. The effect of dependent joints to the ranges-of-motion (ROMs) of the model is investigated and compared to the anatomical one. The index, middle, ring and little finger solutions to forward and inverse kinematics problems are then acquired. The implementation of the model, based on the median male bones dimensions, is made available in the open-source Robot Operating System (ROS) framework. ***Results:*** By including additional four inclination angles per finger, the devised kinematic hand model encompasses also finger curvatures, resulting in significant positioning accuracy improvements compared to the conventional model. The used 3D spatial position improvement metrics are the mean absolute (MAE) and mean relative errors (MRE). The dependent joint position MAEs range from 0.22 to 0.34 cm, while MREs range from 2.8 and 3.5 %, whereas the highest absolute and relative errors during fingertip positioning can reach 0.5 cm and 10.5 %, respectively. ***Conclusion:*** The performed investigation allowed establishing that by modelling finger curvature and assuring the adaptability of the model to a variety of human hands and rehabilitation modalities through joint dependency, represents the best approach towards a relatively simple and applicable rehabilitation model with functional human-like hand movements.

Keywords: hand bones; hand joints; range of motion, articular; rehabilitation; robotics; software

Sažetak. ***Cilj*:** U radu se prezentira metoda za razvoj pojednostavljenog ali učinkovitog kinematičkog modela ljudske ruke koji će se implementirati u rehabilitacijskoj robotici. ***Materijali i metode:*** Pristup se temelji na pojednostavljenju postojećeg modela koji ima 24 stupnja slobode gibanja (DOF) na 9 DOF-a, uz uvođenje dodatnih konstrukcijskih parametara, specifičnih za različite vrste hvata. Nakon što je istražen utjecaj ovisnih zglobova na raspon pokreta (ROM) modela, te je isti uspoređen s anatomskim modelom, dobivena su rješenja problema inverzne i direktne kinematike kažiprsta, srednjeg prsta, prstenjaka i malog prsta. Implementacija modela, temeljena na dimenzijama muških kostiju koje odgovaraju medijanu muške populacije, ostvarena je pomoću programskog okruženja otvorenog koda *Robot Operating System* (ROS). ***Rezultati:*** Uzimanjem u obzir četiriju dodatnih kutova nagiba po prstu, razvijeni model ruke obuhvaća i zakrivljenost prstiju, što omogućuje povećanje točnosti pozicioniranja u usporedbi s konvencionalnim modelom. Kao mjerila za utvrđivanje povećanja točnosti prostornog pozicioniranja, korištene su srednja apsolutna greška (MAE) i srednja relativna greška (MRE). MAE se, ovisno o položaju zgloba, kreće od 0,22 do 0,34 cm, dok se MRE kreće od 2,8 do 3,5 %. Najveće apsolutne i relativne greške tijekom pozicioniranja vrha prsta mogu, pak, doseći 0,5 cm, odnosno 10,5 %. ***Zaključak:*** Zaključuje se da modeliranje zakrivljenosti prsta i

[*]**Corresponding author:**
Ervin Kamenar, D. Sc.
University of Rijeka, Faculty of Engineering
Vukovarska 58, 51000 Rijeka, Croatia
E-mail: ekamenar@riteh.hr

osiguranje prilagodljivosti modela različitim pacijentima i rehabilitacijskim modalitetima kroz međuovisnost zglobova, predstavlja najbolji pristup dobivanju relativno jednostavnog, primjenjivog i funkcionalnog modela šake.

Ključne riječi: kosti šake; opseg pokreta zglobova; programska podrška; rehabilitacija; robotika; zglobovi šake

A lower complexity modular hand kinematic model, targeted for use in rehabilitation, including finger inclination angles, is developed.

INTRODUCTION

Human hand kinematics and dynamics, while researched by many, still constitute a problem of great importance for applications in prosthetic design, teleoperation, detailed musculoskeletal study as well as in rehabilitation robotics[1-6]. In fact, with the inherent complexity of the hand, its wide ranges-of-motion (ROMs) and the many grasping capabilities, it is difficult to find a suitable model to adequately describe hand kinematics while matching the intended use of the model itself.

With the aim of improving the control of a prosthetic hand, the real-time visualisation of hand kinematics using a data glove is analysed in[7]. At the Delft university the complete biomechanical 23 degrees-of-freedom (DOFs) hand and wrist model has, in turn, been developed, including the respective kinematics, dynamics and hand synergies, while incorporating muscles and tendons for force generation[8]. The primary use of the developed, but still complex model, is the study of grasping and object manipulation. Based on anatomical data, the recent detailed hand model[9] merges the muscles and bones into a complex full hand musculoskeletal model. In[10] a full musculoskeletal model of the upper extremity, including thumb and index fingers and using bones dimensions of a 50th percentile male, is implemented and made publicly available via the OpenSim simulation software. In another approach to hand modelling proposed in[11], some considerations on finger inclination angles are encompassed, mainly considering interphalangeal and metacarpophalangeal inclinations; the developed model neglects, however, the effects of the palmar arc on the index and middle finger positioning, and introduces additional DOFs to thumb kinematics, resulting in a complex 24 DOFs hand representation. A rather promising simplification of the 24 DOFs hand model to a 9 and a 6 DOFs implementation is proposed in[12]. A similar idea to the latter solution is applied in this paper, but with several major redefinitions and corrections.

The aim of this comprehensive study is the development of the functional forward and inverse kinematics model of four human fingers, excluding the thumb, and the open-source implementation of the respective modular hand model to be used in rehabilitation robotics, tailored at rehabilitating particular grasp types. The Robot Operating System (ROS), a widely used and community developed and maintained open-source framework for prototyping robotic applications, is used in this frame. The developed model represents a good compromise between the complex solutions, leaning towards biomechanical research, and the oversimplified ones, aimed at purely robotics applications. To our knowledge, no such implementation is available in literature.

MATERIALS AND METHODS

An approach based on the synthesis of the available musculoskeletal hand model proposed in[10], encompassing inter- and intra-joint constraints for the different hand gestures in the activities of daily living (ADL)[12], is applied in this work. The resulting kinematic model is described by a chain-like structure using rigid links, representing the bones, mutually connected with movable joints. The movable revolute joints coincide herein with the human joints and enable the angular relative motions among the links. A full 24 DOFs model of the human hand is used first, where the thumb (T) comprises 4 DOFs, while the index (I), middle (M), ring (R) and little (L) fingers comprise 5 DOFs each. The thumb's kinematic chain begins with the trapeziometacarpal (TMC) joint flexion and extension (FE), in addition to its abduction and adduction (AA). It is followed by the metacarpophalangeal (MPC) FE and interphalangeal (IP) FE. The index, middle, ring and little fingers are,

in turn, modelled by using the same kinematic chain consisting of the carpometacarpal (CMC) FE, the metacarpophalangeal (MCP) AA and FE, the proximal interphalangeal (PIP) FE and the distal (DIP) interphalangeal FE.

It is important to emphasize here that the finger joints are mutually dependant, inferring that the independent actuation of each joint, without considering the respective inter- and intra-joint correlations, as implied in the above 24 DOFs hand model, results in an excessive redundancy. A compromise between the exact motion replication and complexity is, therefore, needed.

In section 2.1, a general form of the dependent motion and the case-by-case motion constraints for the common grasping types are introduced. The effect of the introduced coupled joint motions on finger ROMs is elaborated in section 2.2. In section 2.3, an approach to the kinematic description of the index finger and the thus necessary approximations is described; its forward kinematics is then presented in section 2.4, while the respective inverse kinematics in described in section 2.5. The whole hand model implementation is finally introduced in section 2.6.

Simplification by introducing dependency constraints

To perform the needed model simplifications, a study of the motions of the joints during a certain grasp type is necessary. The adopted grasps taxonomy is a conventional one according to[13], while the respective study of the inter- and intra-joint constraints for hand gesture recognition was performed by[12] using a glove that enables the monitoring of the joint angles for a specified hand pose. While the study reported in[12] focuses on hand gestures only, the obtained joints' constraints are generalized in this paper to the overall joints' trajectories. According to the traditional grasp classification, power and precision grasps can then be identified, and each of them split into the corresponding circular and prismatic grasping. In fact, taking into consideration the findings presented in[12], it can be concluded that there exists a slight difference between circular and prismatic grasping. Consequently, different dependency equations will be adopted in this work.

The dependency constraints12, mostly referencing to the IP FE for the thumb and the DIP FE for the other fingers, are rewritten to reference the MCP FE. The basis for such a formulation is that the MCP joint is the first joint in the kinematic chain with a large ROM, and thus has the largest influence on the position of all subsequent joints. Small errors in its approximations result, therefore, in far larger errors in the final pose approximation. All the following dependency constraints are then expressed in the linear form:

$$\theta_{\text{dependent}}[^\circ] = K\theta_{\text{parent}}[^\circ] + B[^\circ] \tag{2.1}$$

where $\theta_{dependent}$ is the angular position of the dependent joint, θ_{parent} is the angular position of the parent joint, while K denotes slope, and B the intercept of the linear dependency.

Using only slope will be sufficient in most of the following equations to attain a valid representation. The thumb is then completely decoupled from the rest of the fingers, its TMC AA motion is independent, whereas its TMC and IP FE can be constrained to the MCP FE motion. The TMC FE has a different reference position in the musculoskeletal model[10] and the simplified hand model[12], so that an additional offset of -45° has to be added to the intra-joint dependency equation, resulting in the following form, valid for both the prismatic and the circular grasping:

$$\theta_{\text{T,TMC,FE}} = \frac{11}{10}\theta_{\text{T,MCP,FE}} - 45^\circ \tag{2.2}$$

$$\theta_{\text{T,IP,FE}} = \frac{5}{4}\theta_{\text{T,MCP,FE}} \tag{2.3}$$

Although it is well known that the PIP and the DIP joint motions for the I, M, R and L fingers are strongly coupled, in this research an additional simplification, according to[12], is introduced, relating the PIP and DIP flexions and extensions to the MCP joint, thus effectively reducing the dimensionality of the problem. For circular grasping, the constraints can therefore be expressed as:

$$\theta_{i,\text{PIP,FE}} = K_{i,\text{PIP}}\theta_{i,\text{MCP,FE}} = \frac{3}{4}\theta_{i,\text{MCP,FE}} \quad \forall\, i \in \{\text{I, M, R, L}\} \tag{2.4}$$

$$\theta_{i,\mathrm{DIP,FE}} = K_{i,\mathrm{DIP}}\theta_{i,\mathrm{MCP,FE}} = \frac{1}{2}\theta_{i,\mathrm{MCP,FE}} \quad \forall\, i \in \{\mathrm{I,M,R,L}\} \tag{2.5}$$

While performing abduction/adduction, due to common tendons, an additional relationship exists between both the middle and the index, as well as the little and the ring finger[12]:

$$\theta_{\mathrm{M,MCP,AA}} = \frac{1}{5}\theta_{\mathrm{I,MCP,AA}} \tag{2.6}$$

$$\theta_{\mathrm{R,MCP,AA}} = \frac{1}{2}\theta_{\mathrm{L,MCP,AA}} \tag{2.7}$$

What is more, the palmar arc is simulated using the CMC joints, and the CMC FEs of the index, the middle and the ring fingers are linked to little finger's CMC FE with the largest ROMs so that[12]:

$$\theta_{\mathrm{I,CMC,FE}} = \theta_{\mathrm{M,CMC,FE}} \tag{2.8}$$

$$\theta_{\mathrm{M,CMC,FE}} = \frac{1}{2}\theta_{\mathrm{R,CMC,FE}} \tag{2.9}$$

$$\theta_{\mathrm{R,CMC,FE}} = \frac{2}{3}\theta_{\mathrm{L,CMC,FE}} \tag{2.10}$$

The rest of joints' parameters are independent, dictating the kinematics of the simplified 9 DOFs hand model so that the 3 DOFs defining the AAs are $\theta_{\mathrm{T,TMC,AA}}$, $\theta_{\mathrm{I,MCP,AA}}$ and $\theta_{\mathrm{L,MCP,AA}}$, the 5 DOFs for the FEs are $\theta_{i,\mathrm{MCP,FE}}$ $\forall\, i \in \{\mathrm{T, I, M, R, L}\}$, while the single DOF for the palmar arc is $\theta_{\mathrm{L,CMC,FE}}$. To model the prismatic gestures, when the flexion of the index, the thumb and the middle fingers is slightly less pronounced, these independent joint parameters can still be used, but the thumb IP to MCP FE dependency of equation (2.3) needs to be rewritten as:

$$\theta_{\mathrm{T,IP,FE}} = \frac{5}{6}\theta_{\mathrm{T,MCP,FE}} \tag{2.11}$$

while the PIP and DIP FEs for the index and the middle fingers, as defined in the equations (2.4) and (2.5), are to be modified to the following form:

$$\theta_{i,\mathrm{PIP,FE}} = K_{i,\mathrm{PIP}}\theta_{i,\mathrm{MCP,FE}} = \frac{2}{3}\theta_{i,\mathrm{MCP,FE}} \quad \forall\, i \in \{\mathrm{I,M}\} \tag{2.12}$$

$$\theta_{i,\mathrm{DIP,FE}} = K_{i,\mathrm{DIP}}\theta_{i,\mathrm{MCP,FE}} = \frac{1}{3}\theta_{i,\mathrm{MCP,FE}} \quad \forall\, i \in \{\mathrm{I,M}\} \tag{2.13}$$

The DIP and PIP to MCP relations of equations (2.4) and (2.5) hold for the ring and the little finger during both the prismatic and the circular grasping as well.

Another herein considered modality, is the rehabilitation on the finger-by-finger basis. In this case the flexion of one finger invokes an additional involuntary flexion of one or more neighbouring fingers, expressed by inter-finger constraints[12]. While exercising the index finger only, the middle finger then flexes according to[12]:

$$\theta_{\mathrm{M,MCP,FE}} = \frac{1}{5}\theta_{\mathrm{I,MCP,FE}} \tag{2.14}$$

while, in turn, exercising the middle finger, the ring finger flexes according to[12]:

$$\theta_{\mathrm{R,MCP,FE}} = \frac{2}{3}\theta_{\mathrm{M,MCP,FE}} \tag{2.15}$$

Finally, while exercising the ring finger, the middle and the little fingers flex conforming to the linear inequalities as described in[12]. These can be linearized across the MCP FE ROM in the range between [-10°, 90°] so that:

$$\theta_{\mathrm{M,MCP,FE}} = \frac{1}{3}\theta_{\mathrm{R,MCP,FE}} \tag{2.16}$$

$$\theta_{\mathrm{L,MCP,FE}} = \frac{4}{9}\theta_{\mathrm{R,MCP,FE}} \tag{2.17}$$

Joint dependency effect on the ROMs

The introduction of the joint dependency constraints to the human arm model induces an effect on the ranges-of-motion that must be further investigated and compared to the anatomical limits of the joints. The ROM of each joint must therefore not exceed the anatomical limits during an exercise, since rehabilitation is a safety-critical activity and overextension could cause straining injuries, as well as patient discomfort. The anatomical static joint ROMs are adopted here from[10, 14].

Since MCP is used as a parent for most dependencies, implementing the MCP joint constraints indirectly defines the available ROMs of the PIP,

Table 1. Intra-joint FE dependency ROMS

Finger FE		*K* [/]	*B* [°]	LB [°]	UB [°]	LBD [°]	UBD [°]
Thumb	MCP (parent)	-	-	0	65	-	10
	TMC (dependent)	1.1	-45	-45	26.5	-	3.5
	IP (dependent)	1.5	-	0	81.25	-	-
Circular I, M, R, L	MCP (parent)	-	-	-10	90	-20	-
	PIP (dependent)	0.75	-	-7.5	67.5	-	25
	DIP (dependent)	0.5	-	-5	45	-	35
Prismatic I, M	MCP (parent)	-	-	-10	90	-20	-
	PIP (dependent)	0.6	-	-6.6	60	-1	32.5
	DIP (dependent)	0.3	-	-3.3	30	-1.5	50

FE – flexion/extension, ROMs – ranges-of-motion, *K* – slope, *B* – intercept, LB – lower bound, UB – upper bound, LBD – lower bound deficit, UBD – upper bound deficit, I – index, M – middle, R – ring, L – little, MCP – metacarpophalangeal, TMC – trapeziometacarpal, IP – interphalangeal, PIP – proximal interphalangeal, DIP – distal interphalangeal

Table 2. Inter-finger AA dependency ROMs

Finger AA	*K* [/]	LB [°]	UB [°]	LBD [°]	UBD [°]
I – MCP (parent)	-	-15	15	-15	15
M – MCP (dependent)	0.2	-3	3	-17	17
L – MCP (parent)	-	-15	15	-10	10
R – MCP (dependent)	0.5	-7.5	7.5	-15	15

AA – abduction/adduction, ROMs – ranges-of-motion, K – slope, LB – lower bound, UB – upper bound, LBD – lower bound deficit, UBD – upper bound deficit

Table 3. Palmar arc dependency (CMC FE) ROMs

CMC FE	*K* [/]	LB [°]	UB [°]	LBD [°]	UBD [°]
L (parent)	-	0	15	-	-
R (dependent, parent: L)	0.6	0	10	-	-
M (dependent, parent: R)	0.5	0	5	-	-
I (dependent, parent: M)	1	0	5	-	-

CMC – carpometacarpal, FE – flexion/extension, ROMs – ranges-of-motion, *K* – slope, LB – lower bound, UB – upper bound, LBD – lower bound deficit, UBD – upper bound deficit, I – index, M – middle, R – ring, L – little

DIP, TMC and IP joints. For the same reason, during FE, the MCP ROM must be narrowed down, as presented in Table 1. During both the circular and the prismatic grasps with the I, M, R and L fingers, the MCP FE has a lower bound deficit (LBD) in hyperextension of 20°, so that the dependency constraint does not result in PIP and DIP overextensions. The full flexion of the MCP is, in turn, allowed, causing a 25 – 50° upper bound deficit (UBD) in the PIP and DIP ROMs. Considering the thumb MCP, an UBD of 10° exists, which does not cause an excessive flexion in the TMC and IP joints.

By comparing then the inter-finger joint dependencies during AA, presented in Table 2, the ROMs are significantly reduced, with the lower and upper bound deficits of ~ 15°. These deficits are introduced to prevent the possibility of finger overlapping as well as to allow only slight finger contact, as regularly occurring during grasping. The overlapping of fingers can then be trained in the finger-by-finger modalities.

Finally, during the arch-like motion of the palm, the CMC FE of the little finger is the highest, and the complete ROM is covered for the L, R, M and I fingers (Table 3).

Kinematic characterisation of the index finger

The kinematic description of the index finger, with a simplified geometry, and considering 8 finger-specific parameters, is introduced next. The analysis is based on the index finger, but the same procedure can also be applied to the R, M and L fingers, obtaining an equivalent model with different values of the constituting parameters.

According to[10], the neutral position of the finger is defined as the position where the long axes of the phalangeal and the metacarpal bones align. To completely replicate finger's motion in a 3D space, it is then necessary to position all the joint centres of rotation in space, making the model extremely complex. Consequently, the concept of approximation planes, as depicted in Figure 1, is introduced. The hypothesis here is that the accuracy of the model will not be severely impacted if, instead of the rotational centres in 3D space, their projections on finger's FE approximation planes are used. The FE approximation plane is defined herein as the plane where the finger CMC joint and the fingertip (TIP) points lie, while its normal coincides as much as possible with all the FE rotational joint axes adopted from[10]. The finger AA plane is, in turn, defined as the plane perpendicular to the FE plane, where the AA motion occurs.

The kinematic model described in[12] implies the complete straightness of finger's kinematic chain in all the views. Such implementation, although valid for simple applications, does not take into due consideration the additional angles between the kinematic links in finger's neutral position. Due to the inclinations of the rotational centres, these angles are induced by the articular surfaces at the ends of the phalangeal bones responsible for rotational motions. To mitigate the errors introduced by finger's straightness to its spatial localization, an additional finger curvature is considered by introducing the β_1, β_2, β_3 and β_4 inclination angles in the FE plane (Figure 2). In Figure 2 are depicted the geometrical parameters of the index finger in the two approximation planes, where L_1, L_2, L_3 and L_4 denote the distances between the neighbouring joint centres of rotation.

Due to the large number of used symbols, in this Figure, as in the remainder of the paper, the previously established naming convention of the five joint parameters is simplified, so that the index *i*, denoting finger type, is omitted. The curvature of the finger in the AA plane is then neglected due to the small measured inclination angles influencing just slightly the DIP and PIP positions, without shifting the TIP position. The measured values of the index finger-specific parameters of Figure 2, that will be used for the visual validation of the

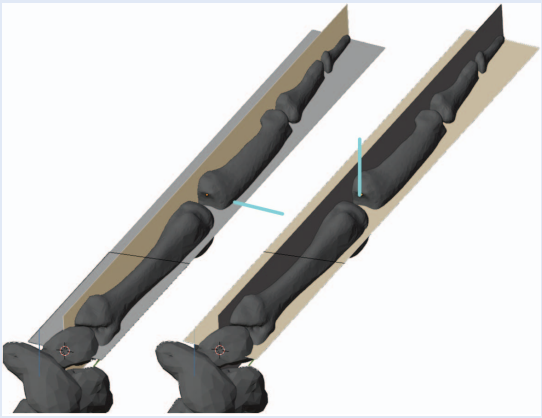

Figure 1. Index finger AA (left) and FE (right) approximation planes and their normals (light blue)

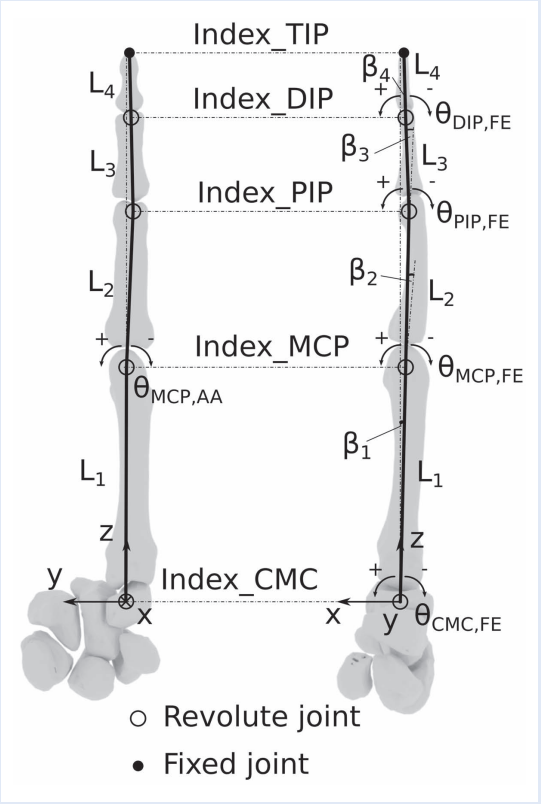

Figure 2. Kinematic description of index finger in FE and AA approximation planes

Table 4. Finger-specific parameters for index finger measured from 50th percentile male model

Finger parameters	L_1 [cm]	L_2 [cm]	L_3 [cm]	L_4 [cm]	β_1 [°]	β_2 [°]	β_3 [°]	β_4 [°]
Measured value	6.34	4.26	2.51	1.80	2	0	7	-3

results, are reported in Table 4. To generalize further the model and enable its fitting to different individuals, the phalange-to-hand length ratios can be assumed here as those proposed in[9, 15]. It is important to note, however, that they represent phalange lengths, and not joint-to-joint revolution axes distances (the mentioned L_i values), resulting, thus, in slightly different values.

Forward kinematics – modified Denavit-Hartenberg convention

Having described in the above treatise the geometric parameters of the I, M, R and L fingers, the problem of fingers' motion in 3D space can be tackled next. The forward kinematics solution positions then each finger in the local coordinate system by using three rotations and three positions. To calculate these positions, all joint parameter values ($\theta_{CMC,FE}$, $\theta_{MCP,FE}$, $\theta_{MCP,AA}$, $\theta_{PIP,FE}$, $\theta_{DIP,FE}$) have to be known. The joints representation is simplified here by assuming that the joints are revolute; the resulting kinematic tree consists hence of a revolute joint, representing the CMC FE, a universal joint, representing the MCP FE and AA, and two additional revolute joints, for the PIP and the DIP FE representations. To comply with the convention stating that a single joint must be represented by a single DOF only, the MCP universal joint is represented using two revolute joints, where the arrangement of these joints is of paramount importance.

The schematic representation of the correct and the incorrect joint arrangement is depicted in Figure 3a. In contrast to the arrangement adopt-

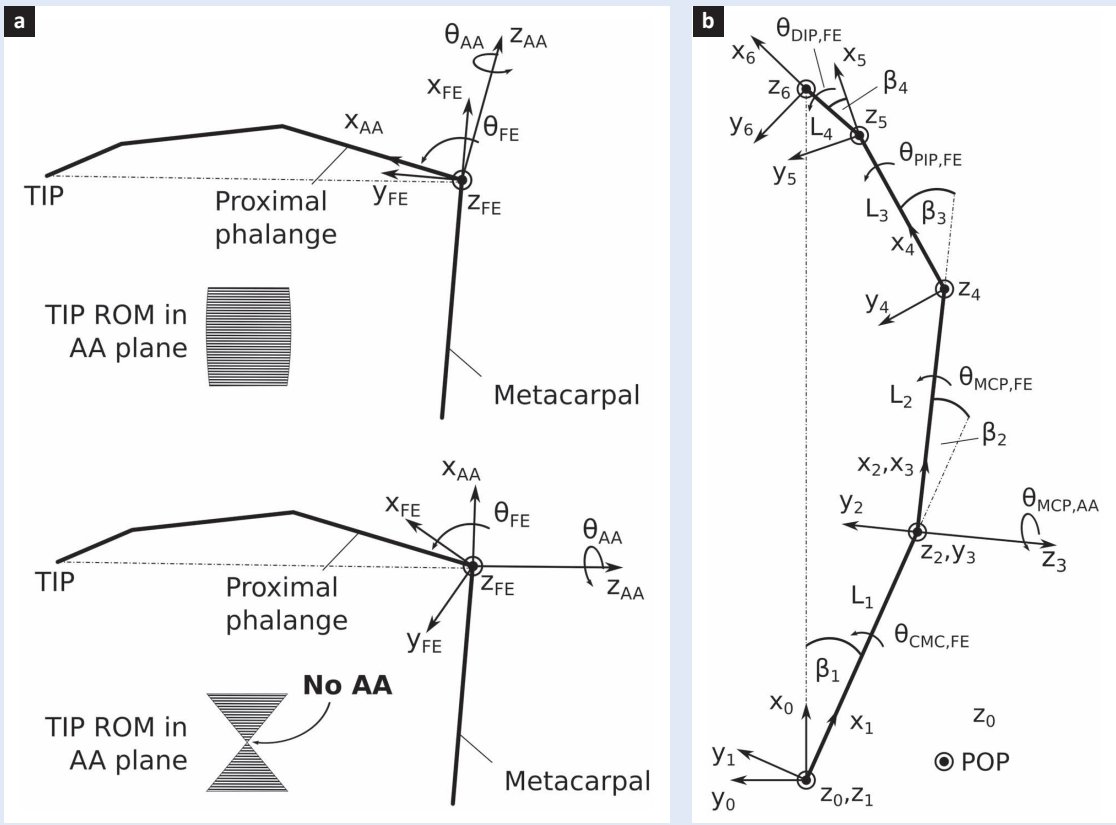

Figure 3. The MCP joint ordering considerations (a) and the modified DH forward kinematics convention for the I, M, R and L fingers in the FE plane (b)

ed in[12], the MCP FE must, in fact, precede MCP AA, so that the AA axis of revolution (labelled in the Figure with Z_{AA}) revolves with the proximal phalange, functionally representing the ROM of the real finger. If such ordering is not used, at a certain angle the finger's TIP and the Z_{AA} axis align, and the finger revolves around its axis, decreasing its ROM around the flexion angle. Such phenomenon does not, obviously, occur during the factual finger motion. To condense, the AA axis of revolution must rotate during the MCP FE together with the proximal phalange.

In Figure 3b the frames and the parameters necessary to describe the forward kinematics behaviour of the I, M, R and L fingers are presented. The inclination angles β_i of the finger are intentionally exaggerated here for clarity reasons. The shown frames are obtained by using the widely accepted modified Denavit-Hartenberg (DH) notation[16]. This procedure can be split into three main parts: attaching frames to the links, determining the parameters of the four links, and obtaining the homogenous transformation matrix representing the 6D position and orientation of the TIP in the base frame coordinate system.

Since no prismatic joints are present in this finger representation, the DH procedure will be clarified on an all-revolute configuration. The frames are considered here as rigidly attached to the assigned links, so that the shifts of the links, caused by the rotations of the joints, result in an identical shift in the position of the frame. The z_i-axis of the frame corresponds to the axis of revolution of *i*-th joint, with the adopted attachment procedure as described in[16]. By attaching the frames to the links, the modified DH finger parameters reported in Table 5 are determined so that[16]:

- a_{i-1} represents the distance along the x_{i-1} axis from the z_{i-1} to the z_i axis;
- α_{i-1} represents the angle about the x_{i-1} axis measured from the z_{i-1} to the z_i axis;
- d_i represents the distance along the z_i axis from the x_{i-1} to the x_i axis;
- θ_i represents the angle about the z_i axis measured from the x_{i-1} to the x_i axis.

In the final step, the homogenous transformation matrices are acquired by inserting the modified DH parameters from Table 5 to the general transformation matrix T_i^{i-1}, consisting of a 3 × 3 rotational matrix R_i^{i-1} and a 3 × 1 translation vector P_i^{i-1}. The general form of the matrix is acquired via two screw-like transforms, i.e., the translation along a_{i-1} and a rotation about a_{i-1}, followed by the translation along d_i and the rotation about θ_i:

Table 5. Modified Denavit-Hartenberg parameters

Link	α_{i-1}	a_{i-1}	d_i	θ_i
1	0	0	0	$\theta_{CMC,FE} - \beta_1$
2	0	L_1	0	$\theta_{MCP,FE} - \beta_2$
3	π/2	0	0	$\theta_{MCP,AA}$
4	− π/2	L_2	0	$\theta_{PIP,FE} + \beta_3$
5	0	L_3	0	$\theta_{DIP,FE} + \beta_4$
6	0	L_4	0	0

$$T_i^{i-1} = \begin{bmatrix} R_i^{i-1} & P_i^{i-1} \\ 0 \quad 0 \quad 0 & 1 \end{bmatrix} = \\ = \begin{bmatrix} c_{\theta_i} & -s_{\theta_i} & 0 & a_{i-1} \\ s_{\theta_i} c_{\alpha_{i-1}} & c_{\theta_i} c_{\alpha_{i-1}} & -s_{\alpha_{i-1}} & -d_i s_{\alpha_{i-1}} \\ s_{\theta_i} s_{\alpha_{i-1}} & c_{\theta_i} s_{\alpha_{i-1}} & c_{\alpha_{i-1}} & d_i c_{\alpha_{i-1}} \\ 0 & 0 & 0 & 1 \end{bmatrix} \tag{2.18}$$

In this and all subsequent matrices, the following symbols are used to simplify as much as possible the used notation:

$$(c_{\theta_i}, c_i) \Longrightarrow \cos\theta_i \,;\; (s_{\theta_i}, s_i) \Longrightarrow \sin\theta_i \\ for \;\; i \in [1,6] \tag{2.19}$$

$$c_{\alpha_{i-1}} \Longrightarrow \cos\alpha_{i-1} \,;\; s_{\alpha_{i-1}} \Longrightarrow \sin\alpha_{i-1} \\ for \; i \in [1,6] \tag{2.20}$$

Six resulting matrices (T_0^1, T_1^2, T_2^3, T_3^4, T_4^5, T_5^6) describe the transformations between neighbouring frames according to Figure 3. The position and orientation of each frame with respect to the base frame is attained next via the multiplications of the matrices. To avoid human errors, these multiplications are performed, and the obtained results are simplified by introducing trigonometric relations, using the library for symbolic mathematics *sympy*[17], written in the *Python* programming language.

Since the rehabilitation problem is not only about controlling the trajectory of the tip of the finger,

but also of all the joints in motion, the homogenous transformation matrices, positioning the MCP FE (T_2^0) and AA (T_3^0), as well as the PIP (T_4^0) and DIP (T_5^0), are also of great importance. All these matrices are available in open access in authors' GitHub repository[18], while the final homogenous matrix for the TIP of the finger is:

The model is implemented in the open-source framework with intra-finger joint constraints and couplings, resulting in a significant improvement in fingertip spatial positioning with significantly reduced mean relative positioning errors.

$$T_6^0 = T_1^0 T_2^1 T_3^2 T_4^3 T_5^4 T_6^5 = \begin{bmatrix} c_{12}c_3c_{45} - s_{12}s_{45} & -c_{12}c_3s_{45} - c_{45}s_{12} & -c_{12}s_3 & a_1c_1 + a_3c_{12}c_3 + a_4(c_{12}c_3c_4 - s_{12}s_4) + a_5(c_{12}c_3c_{45} - s_{12}s_{45}) \\ c_{12}s_{45} + c_3c_{45}s_{12} & c_{12}c_{45} - c_3s_{12}s_{45} & -s_{12}s_3 & a_1s_1 + a_3c_3s_{12} + a_4(c_{12}s_4 + c_3c_4s_{12}) + a_5(c_{12}s_{45} + c_3c_{45}s_{12}) \\ c_{45}s_3 & -s_3s_{45} & c_3 & s_3(a_3 + a_4c_4 + a_5c_{45}) \\ 0 & 0 & 0 & 1 \end{bmatrix} \quad (2.21)$$

Numerical approach to the inverse kinematics solution

For the full finger kinematics implementation in a robotic system, forward kinematics constitutes just part of the description. The inverse kinematics (IK) problem, needed to determine the parameters of the joints of the finger ($\theta_{CMC,FE}$, $\theta_{MCP,FE}$, $\theta_{MCP,AA}$, $\theta_{PIP,FE}$, $\theta_{DIP,FE}$), if the 6D position of the TIP, as described by the matrix (2.21), is known, is equally important:

$$T_6^0 = \begin{bmatrix} & R_6^0 & & P_6^0 \\ 0 & 0 & 0 & 1 \end{bmatrix} = \begin{bmatrix} r_{11} & r_{12} & r_{13} & p_x \\ r_{21} & r_{22} & r_{23} & p_y \\ r_{31} & r_{32} & r_{33} & p_z \\ 0 & 0 & 0 & 1 \end{bmatrix} \quad (2.22)$$

To speed up the motion planning algorithms, the problem of solving an overdetermined nonlinear system with 6 equations and 5 unknowns is approached numerically, by using a custom *sympy* script and the *scipy*[19] least-squares solver. To reduce the complexity of the problem, as well as the number of DOFs, a general dependency equation, linking the DIP and PIP FEs to the MCP FE, as per equations (2.4) and (2.5), is employed. The K_{PIP} and K_{DIP} coefficients are hence introduced to the homogenous matrices T_1^0, T_2^0, T_3^0, T_4^0, T_5^0 and T_6^0. In the resulting overdetermined system of equations, the three unknown finger joint parameters $\theta_{CMC,FE}$, $\theta_{MCP,FE}$ and $\theta_{MCP,AA}$ have to be computed from the six equations defining the transformation matrix, three relating to the rotations and the remaining three to the respective linear coordinates.

Two different solving techniques are tried. First, an entire transformation matrix T_6^0 is used, while in the next step just the P_6^0 position vector is employed – in both cases with the aim to obtain an approximate solution to the three unknown finger joint parameters. The rationale behind using the position vector only, is to speed up the calculations by performing fewer evaluations. An additional increase of the speed is secured by using an analytically obtained Jacobian matrix from the position vector contained in expression (2.21), which reduces the number of numeric approximations of the first-order partial derivatives of P_6^0 with respect to the three unknown joint parameters. The columns of the Jacobian are obtained herein by introducing in the expression (2.21) the DH parameters from Table 5, the K_{PIP} and K_{DIP} coefficients of equations (2.4) and (2.5), and then performing symbolic differentiation. The columns of the Jacobian $\frac{\partial}{\partial \theta_{MCP,AA}} P_6^0$, $\frac{\partial}{\partial \theta_{MCP,FE}} P_6^0$, and $\frac{\partial}{\partial \theta_{CMC,FE}} P_6^0$ along with the whole calculation flow, are again available in open access in authors' GitHub repository[18].

During the calculations, the parameters of the joints are constrained according to the dependencies given in Tables 1, 2 and 3, the initial guess is set to 0°, while the termination tolerance for the change of the unknown parameters, obtained iteratively bearing in mind computational speed, is set to 10^{-5}. The resulting average execution time while using the entire transformation matrix is ~ 21 ms, with the time needed for the computation of the position vector and the ana-

lytical Jacobian being ~ 13 ms. Using only the position vector and the analytical expression for the Jacobian reduces the calculation time by ~ 38 %, both times aligning well with the average IK times reported in literature[20].

To validate both numerical techniques, a grid of 40 × 40 × 40 (64,000 in total) joint parameter values, spaced evenly between the upper and lower bounds (Tables 1, 2 and 3), is generated first. By using the transformation matrix (2.21), forward kinematics is then calculated over the entire grid, resulting in the rotation matrix R_6^0 and the position vector P_6^0. The inverse kinematics solvers are employed next on the obtained transformation matrix, allowing to attain the resulting joint parameter values, which are finally compared to the input parameter values. While using the entire transformation matrix, the solver reached the desired solution over the entire grid. On the other hand, when only the position vector is used, the matching of the parameter values is reached in ~ 98 % of the cases. In the remaining ~ 2 % of the cases, the position of the TIP of the finger is close to the neutral position, where different combinations of $\theta_{CMC,FE}$ and $\theta_{MCP,FE}$ can result in approximately the same TIP positions in the 3D space. If the orientation of the transformation matrix is excluded, in the proximity of the finger neutral position the solver can also converge to several alternative solutions. Considering all these aspects, it can be asserted that the validity and applicability of the numerical IK solver for the I, M, R and L fingers is successfully confirmed.

Open-source implementation of the hand kinematics model

As basis for hand rehabilitation (Figure 4), the implementation of the developed kinematics model is performed by using the ROS ecosystem and its Unified Robot Description Format (URDF). In this frame, the adopted bone structure is that corresponding to a median male as proposed in[10]. The principle of approximation planes is employed for each finger separately, while paying attention as much as possible to the correspondence with all the finger joints' axes of revolutions. The revolution axes are determined here by fitting a cylinder to the articulate joint surface[10], while all the 24 DOFs are incorporated in the model. The axes of rotation of the thumb, are, in turn, determined without making use of the approximation planes[10]. The ROS environment provides the needed flexibility and modularity for the required implementation of the diverse rehabilitation modalities. The resulting implementation of the joint constraints for the rehabilitation sessions according to equations (2.2) – (2.17), while using different

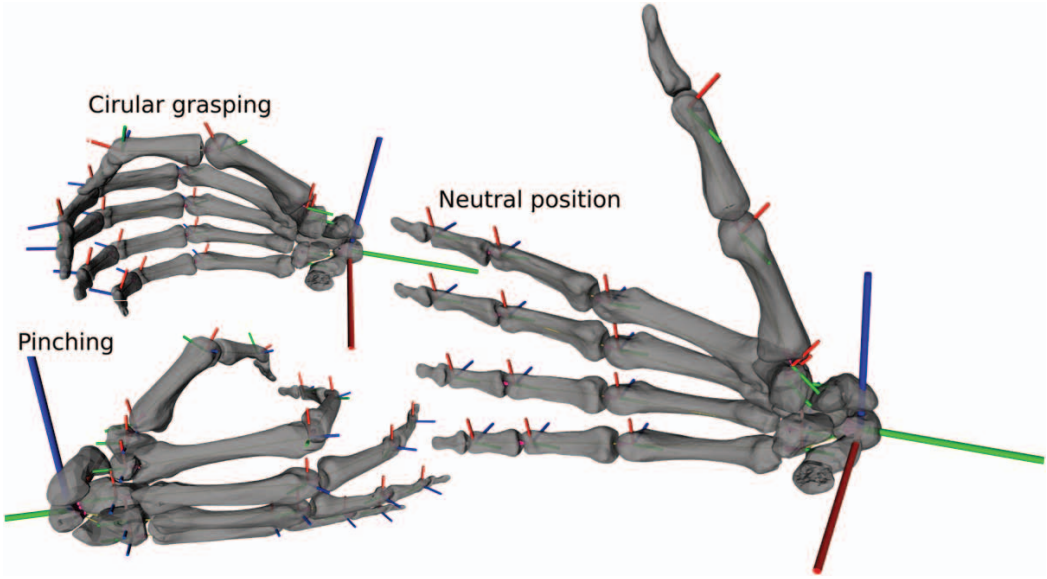

Figure 4. Hand grasp examples (left) and neutral position (right)

models for the circular and the prismatic grasping of the whole hand, as well as for the I, M or R fingers only, is provided in open access in authors' GitHub repository[18]. The inter-finger constraints for the finger-by-finger exercise are then visualised in Figure 5.

The forward kinematics implementation within the scope of the ROS framework, based on transformation trees, is handled in this frame by using the ROS internal tf2 library[21]. The used coordinate frame convention, although adopted from models based on the joint coordinate system established by International Society of Biomechanics[22], is, in turn, modified to match the ROS coordinate conventions as suggested in[23].

Statistics

All the statistical analyses, validations and visualisations are performed in the outlined framework by employing the R statistical programming environment24. Two different error metrics are then used to validate the model: the absolute (AE) and the relative (RE) errors. AE is defined as the Euclidean distance between two position points in the 3D space, $(p_{x\beta}, p_{y\beta}, p_{z\beta})$ and $(p_{x\emptyset}, p_{y\emptyset}, p_{z\emptyset})$:

$$\mathrm{AE} = \sqrt{\left(p_{x\beta}-p_{x\emptyset}\right)^2+\left(p_{y\beta}-p_{y\emptyset}\right)^2+\left(p_{z\beta}-p_{z\emptyset}\right)^2} \tag{2.23}$$

On the other hand, RE is calculated by dividing AE with the distance to the origin:

$$\mathrm{RE} = \frac{\mathrm{AE}}{\sqrt{{p_{x\beta}}^2 + {p_{y\beta}}^2 + {p_{z\beta}}^2}} \tag{2.24}$$

A significance analysis is performed herein by using a linear regression model with interactions, while the used measure of variability is the coefficient of determination R^2. An analysis-of-variance (ANOVA) is performed on the resulting linear regression model to determine if the model terms are significant. The hence used significance level for the test is $\alpha = 0.05$, while the factors are considered statistically significant when the p-values $\leq \alpha$.

For the descriptive statistics of the inter-model errors, the mean value is used as the measure of central tendency, whereas range is used as the measure of the variability.

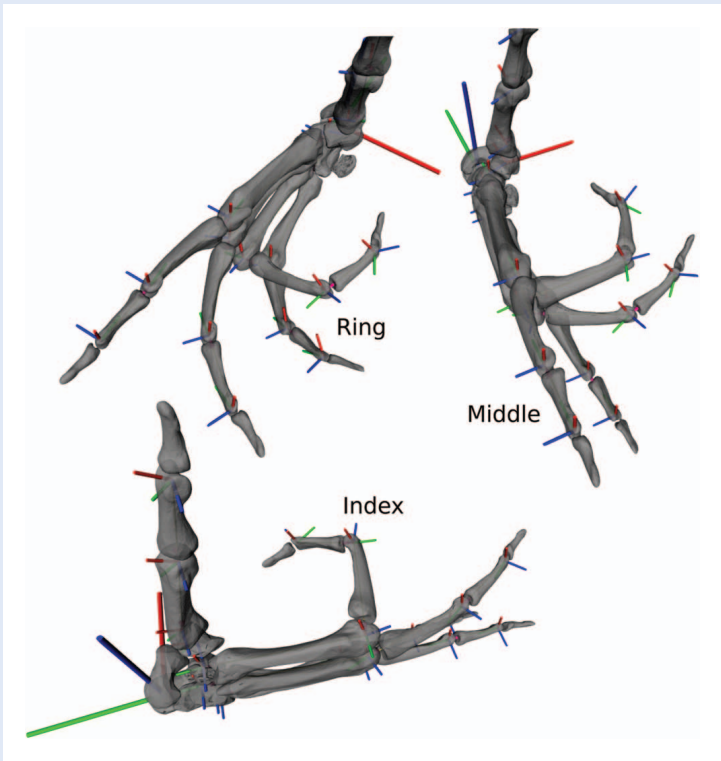

Figure 5. Inter-finger joint constraints for finger-by-finger exercise

RESULTS

For the visual validation of the obtained forward kinematics solutions, the workspace of the index finger is computed. To compute this workspace, only the translation vectors P_i^{i-1}, containing the x, y and z coordinates, are extracted as a subset of each transformation matrix (T_1^0, T_2^0, T_3^0, T_4^0, T_5^0 and T_6^0). The thus attained MCP, DIP, PIP and TIP translation vectors, with substitutions for the joint parameters, are provided once more in authors' GitHub repository[18]. They are evaluated over the 3D "meshgrid" of the values for the joints in the space defined by the index finger constraints, as given for the MCP FE and AA, as well as the CMC FE in Table 1, 2 and 3, respectively, with a step value of 1°. The resulting dataset for the validation comprises 260,000 data points. The L_i dimensions and the β_i angles of the DH parameters are then substituted with the ones given in Table 4, while, by using equations (2.4) and (2.5) for circular grasping, and equations (2.12) and (2.13) for the prismatic one, the $\theta_{\mathrm{PIP,FE}}$ and $\theta_{\mathrm{DIP,FE}}$ dependent joints are expressed in terms of $\theta_{\mathrm{MCP,FE}}$.

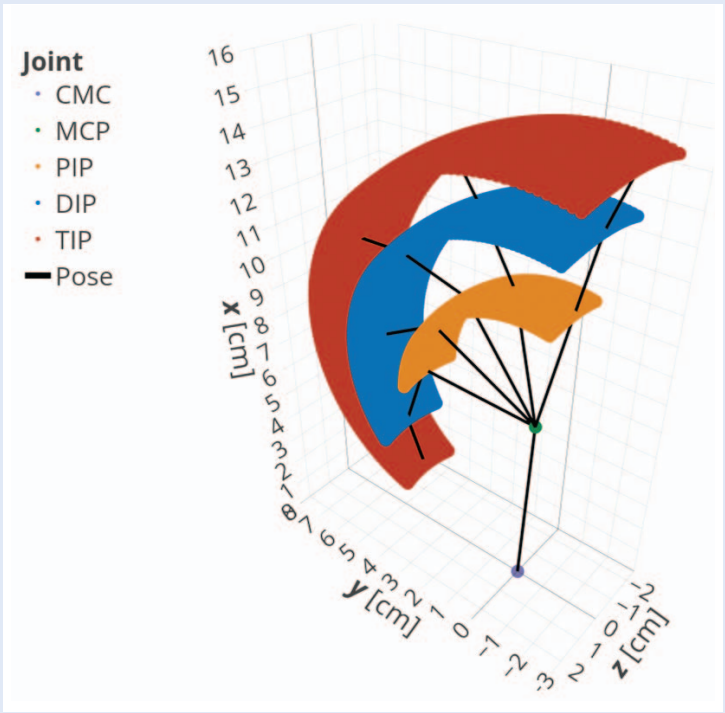

Figure 6. Reachable workspace of the index finger in a 3D space during circular grasping ($\theta_{CMC,FE}$ = 0°)

In Figure 6 are depicted the reachable workspace and the positions of each finger joint (CMC, MCP, PIP, DIP and TIP) for circular grasping in the 3D space. Some of the poses of each finger are represented by black lines. The coupled motion of each joint during the finger FE follows a circular trajectory, while the small palmar arc-like $\theta_{CMC,FE}$ rotations shift the trajectories. The main difference between the possible paths during the circular and prismatic grasping, while taking into due consideration the dependent joint constraints, manifest itself in the slightly larger flexion during circular grasping, resulting in the DIP and TIP positions closer to the palm of the hand in the highest flexion point. From the results shown in Figure 6, it can also be inferred that there is no ROM reduction during AA, which visually validates the proposed finger kinematic model.

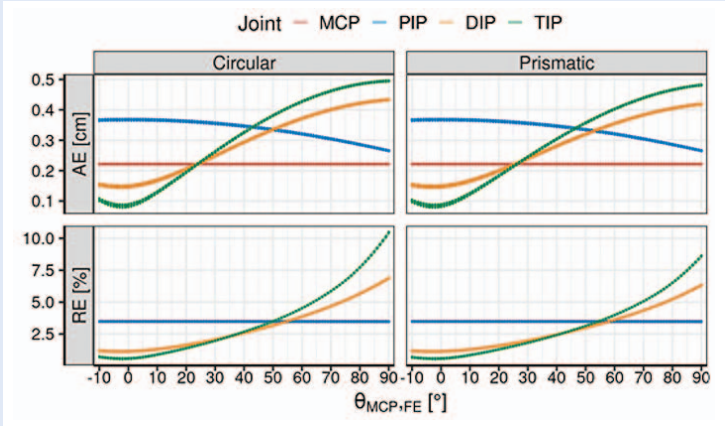

Figure 7. Model comparisons – with ($\beta_i \neq 0$) and without finger curvature ($\beta_i = 0$)

To justify the addition of the finger curvature parameters in the model, the model proposed in[12], where the described corrections are not included, is related to the one proposed in this work. By using the AE and RE metrics, as defined by equations (2.23) and (2.24) respectively, models pertaining to two cases are compared: that with and the one without finger curvature $|(p_{x\beta}, p_{y\beta}, p_{z\beta}$ for $\beta_i \neq 0) - (p_{x0}, p_{y0}, p_{z0}$ for $\beta_i = 0|$, where the considered origin for calculating RE is the CMC joint. For the significance analyses of the inter-model AE, the influence of three joint angles ($\theta_{CMC,FE}$, $\theta_{MCP,FE}$ and $\theta_{MCP,AA}$), of the joint type (0 – 6), and of the grasping type (circular, prismatic), is investigated. The resulting linear model can account for 99.5 % of the total AE variability. The performed ANOVA analysis leads then to the conclusion that only the $\theta_{CMC,FE}$ joint angle, with the joint and grasp types and their interactions, are significant (p-values < 0.001). This rules out the effects of the joint angles $\theta_{CMC,FE}$ and $\theta_{MCP,AA}$ on the inter-model AE. The significant variables are therefore used to visualize the errors in Figure 7. The CMC joint is excluded from this visualization since it rotates around the origin only, and thus it induces no positioning errors. The descriptive statistics of the presented data leads, hence, to the following conclusions:

- For the MCP joint, both the AE and the RE are constant throughout the entire workspace for both grasp types, and are respectively equal to 0.22 cm and 3.5 %.
- For both grasping types, the AE value of the PIP joint slightly decreases (from 0.37 to 0.26 cm) towards greater $\theta_{CMC,FE}$ values, while RE is practically constant at around 3.5 %.
- The DIP and TIP joint errors increase with increasing $\theta_{CMC,FE}$ angle, and are slightly higher for circular grasping.

- The AE for the DIP joint spans from 0.14 to ~ 0.44 cm, with a mean value of ~ 0.29 cm, while the respective RE spans from 1.1 to ~ 6.9 %, with a mean value of ~ 3 %.
- The AE values for the TIP joint has an even larger range of variations, i.e., between 0.08 and ~ 0.5 cm, with a mean value of ~ 0.3 cm, translating to a RE range between 0.5 and 10.5 % (3.5 % mean value).

DISCUSSION

The main motivation for this research was to introduce a simplified, but highly modular and grasp-oriented model of the human hand, comprising all constituent joints, for use in the development of active rehabilitation devices. The introduced simplifications are based on approximating the human joints with revolute ones, as well as on coupling the MCP, PIP and DIP finger motions in a functional manner, hence reducing the overall model complexity. The resulting open-source implementation of the model can be found in the GitHub repository[18].

The proposed model can be applied in both research and clinical practices. In fact, it can be used to improve the rehabilitation process by integrating it with quantitative measurements on parametrised models tailored to individual patients. Comparing patient trajectories on a session-by-session basis enables then tracking and assessing the resulting improvement of motoric functions recovery during the neurorehabilitation process. This can lead to personalised treatments and better long-term outcomes. The obtainment of the model parameters from a large calibrated grasping kinematics data[25] can improve further hand rehabilitation by making the model a leverage to a more robust approach to the design and simulation of rehabilitation devices.

Future work will be directed towards the generalization of the model to different hand dimensions, whereas an experimental setup using stereo imaging and a depth camera will be used to populate the configuration database with more rehabilitation modalities and different joint constraints. An attempt will also be made to solve the described inverse kinematics problem analytically, since such a solution would significantly reduce the computational burden. By using a simulation-before-prototype design approach, a prototype of a hand rehabilitation device for patients suffering from poststroke paresis will thus be developed.

CONCLUSIONS

A simplification process of the full 24 DOFs hand model, where the effect of inter- and intra-finger joint dependency on the resulting ranges-of-motion is evaluated, is presented in this work. The kinematic characterisation of the index finger, generalizable to the middle, ring and little fingers, is also provided, alongside considerations on joints' ordering. A process of obtaining a numerical inverse kinematics solution is illustrated and complemented with detailed procedures for attaining feasible joint parameters. The modularity and availability of the model are assured in this frame through its implementation in the Robot Operating System (ROS).

By neglecting the finger inclination angles, and based on the median male bone dimensions, mean absolute errors (MAE) ranging from 0.22 to 0.34 cm for the different joints of the index finger are introduced in the model, with the highest absolute error rising up to 0.5 cm for TIP position. The mean relative errors (MRE) range, in turn, between 2.8 and 3.5 %, with the highest relative error for the TIP displacement of up to 10.5 %, proving a significant effect of finger curvature on finger's pose.

The main contribution and novelty presented in this paper is the increased precision of the hand kinematics model of four human fingers intended for rehabilitating particular grasp types. What is more, the developed model comprises realistic bones' dimensions, inter- and intra-finger joint constraints and accounts for the curved finger shape. To authors' knowledge, no such flexible open-source model of the human hand, designed for the finger-by-finger as well as for the whole hand rehabilitation modalities, is available at this time.

ACKNOWLEDGMENTS

Work supported by the University of Rijeka, Croatia, grant uniri-tehnic-18-32 "Advanced mechatronics devices for smart technological solu-

tions" and enabled by a far-reaching collaboration and common work with the University of Rijeka, Centre for Micro- and Nanosciences and Technologies and the Clinical Hospital Centre Rijeka, Croatia.

Conflicts of Interest: Authors declare no conflicts of interest.

REFERENCES

1. Peña-Pitarch E, Falguera NT, Yang JJ. Virtual human hand: model and kinematics. Comput Methods Biomech Biomed Engin 2012;17:568–579.
2. Li R, Wang H, Liu Z. Survey on mapping human hand motion to robotic hands for teleoperation. IEEE Trans Circuits Syst Video Technol 2022;32:2647–2665.
3. Bao T, Zhao Y, Zaidi SAR, Xie S, Yang P, Zhang Z. A deep kalman filter network for hand kinematics estimation using sEMG. Pattern Recognit Lett 2021;143:88–94.
4. Ma'touq J, Hu T, Haddadin S. A validated combined musculotendon path and muscle-joint kinematics model for the human hand. Comput Methods Biomech Biomed Engin 2019;22:727–739.
5. Ma'touq J, Hu T, Haddadin S. Sub-millimetre accurate human hand kinematics: from surface to skeleton. Comput Methods Biomech Biomed Engin 2018;21:113–128.
6. de Sousa IM, de Jesus Trindade JL, Pizo GAI. Simulation of human hands movements using forward kinematics. *In:* Costa-Felix R, Carlos Machado J, Alvarenga AV (eds). CBEB 2018: Proceedings of the XXVI Brazilian Congress on Biomedical Engineering; 2019 Oct 21-25; Armação de Buzios, Brazil. Singapore: Springer, 2019;705–710.
7. Sharma MD, Phukan N, Kakoty NM, Sonowal D. Visualization of grasping operations based on hand kinematics measured through data glove. *In*: AIR '17: Proceedings of the Advances in Robotics; 2017 Jun 28 – Jul 2; New Delhi, India. New York: ACM Press, 2017;1–6.
8. Gustus A, Stillfried G, Visser J, Jörntell H, van der Smagt P. Human hand modelling: kinematics, dynamics, applications. Biol Cybern 2012;106:741–755.
9. Engelhardt L, Melzner M, Havelkova L, Fiala P, Christen P, Dendorfer S et al. A new musculoskeletal AnyBody detailed hand model. Comput Methods Biomech Biomed Engin 2020;24:777–787.
10. Holzbaur KRS, Murray WM, Delp SL. A model of the upper extremity for simulating musculoskeletal surgery and analyzing neuromuscular control. Ann Biomed Eng 2005;33:829–840.
11. van der Hulst FPJ, Schatzle S, Preusche C, Schiele A. A functional anatomy based kinematic human hand model with simple size adaptation. *In*: ICRA 2012: IEEE International Conference on Robotics and Automation; 2012 May 14-18; Saint Paul, USA. New Jersey: IEEE, 2012;5123–5129.
12. Cobos S, Ferre M, Sánchez-Urán MÁ, Ortego J, Aracil R. Human hand descriptions and gesture recognition for object manipulation. Comput Methods Biomech Biomed Engin 2010;13:305–317.
13. Cutkosky M. On grasp choice, grasp models, and the design of hands for manufacturing tasks. IEEE Trans Rob Autom 1989;5:269–279.
14. Kapandji IA. The Physiology of the Joints, Volume 1: Upper Limb. 6th Edition. London: Churchill Livingstone, 2007.
15. Buryanov A, Kotiuk V. Proportions of hand segments. Int J Morphol 2010;28:755–758.
16. Craig JJ. Introduction to Robotics: Mechanics and Control. 3rd Edition. Harlow: Pearson Education, 2014.
17. Meurer A, Smith CP, Paprocki M, Čertík O, Kirpichev SB, Rocklin M et al. SymPy: symbolic computing in Python. PeerJ Comput Sci 2017;3:103.
18. Github [Internet]. San Francisco: Hand9DOF, Inc. c2022 [cited 2022 May 17]. Available from: https://github.com/tbazina/rehab/tree/master/kinematics/Hand9DOF/Index.
19. Virtanen P, Gommers R, Oliphant TE, Haberland M, Reddy T, Cournapeau D et al. SciPy 1.0: fundamental algorithms for scientific computing in Python. Nat Methods 2020;17:261–272.
20. Diankov R. Automated construction of robotic manipulation programs. Pittsburgh: The Robotics Institute at Carnegie Mellon University, 2010. PhD thesis.
21. Foote T. The transform library. *In*: TePRA 2013: The 5th Annual IEEE International Conference on Technologies for Practical Robot Applications; 2013 Apr 22-23; Boston, Massachusetts, USA. New Jersey: IEEE, 2013.
22. Wu G, van der Helm FC, Veeger HD, Makhsous M, Roy PV, Anglin C et al. ISB recommendation on definitions of joint coordinate systems of various joints for the reporting of human joint motion-Part II: shoulder, elbow, wrist and hand. J Biomech 2005;38:981–992.
23. ROS.org [Internet]. REP 103 – Standard units of measure and coordinate conventions, c2010 [cited 2022 May 17]. Available from: https://www.ros.org/reps/rep-0103.html.
24. R-project.org [Internet]. Vienna: The R Project for Statistical Computing, c2021 [cited 2022 May 17]. Available from: https://www.R-project.org/.
25. Jarque-Bou NJ, Atzori M, Müller H. A large calibrated database of hand movements and grasps kinematics. Sci Data 2020;7:1–10.